Asociación Argentina
de Mecánica Computacional

Mecánica Computacional Vol XXVII, págs. 2085-2097 (artículo completo)
Alberto Cardona, Mario Storti, Carlos Zuppa. (Eds.)
San Luis, Argentina, 10-13 Noviembre 2008

ON MESH INDEPENDENCE IN DYNAMIC FRACTURE ANALYSIS BY MEANS OF THE DISCRETE ELEMENT METHOD

Jorge Daniel Riera[a], Ignacio Iturrioz[b] and Letícia Fleck Fadel Miguel[c]

[a]*Department of Civil Engineering, Federal University of Rio Grande do Sul, Porto Alegre, Brasil, jorge.riera@ufrgs.br, http://www.engcivil.ufrgs.br*
[b]*Department of Mechanical Engineering, Federal University of Rio Grande do Sul, Porto Alegre, Brasil, ignacio@mecanica.ufrgs.br, http://www-gmap.mecanica.ufrgs.br*
[c]*Department of Mechanical Engineering, Federal University of Rio Grande do Sul, Porto Alegre, Brasil, letffm@ufrgs.br, http://www-gmap.mecanica.ufrgs.br*

Keywords: Fracture Analysis, Discrete Element Method, Mesh Independence, Size Effect.

Abstract. The authors successfully applied the so-called Discrete Element Method (DEM) to determine the dynamic response of concrete and rock structures that fracture under the action of static and dynamic loading. When on account of the size of the model larger elements must be employed, the issue of mesh objectivity must be addressed. In response determinations of structures with initial cracks or high stress gradients, which result in fracture localization, well established procedures lead to results that are mesh independent. However, in elements subjected to approximately uniform stress fields a hitherto unknown problem arises in the analysis of non-homogeneous materials: the need to know a priori the degree of fracturing of the element. This should also affect finite element analysis in cases in which there is no clear fracture localization.

Within this context, in this paper a scheme to circumvent this difficulty is suggested by the authors. The applicability of the proposed solution is tested in several numerical examples involving large concrete or rock structures.

1 INTRODUCTION

The determination of the static or dynamic response of solids by means of numerical methods, such as Finite Differences (FDM), Finite Elements (FEM) or Discrete Elements (DEM) requires the estimation of computational errors, *i.e.*, the sensitivity of the solutions to the size or other features of the mesh adopted in the analysis. In Linear Elasticity problems the issue is commonly addressed by comparing solutions obtained with increasingly finer meshes until convergence is reached with the desired accuracy. In Linear Elastic Fracture Mechanics (LEFM), a similar approach is possibly the only feasible alternative to assess convergence of the solution. The performance of the DEM has been evaluated both in the solution of Linear Elasticity problems as well as in connection with problems of LEFM, as a preliminary step before application of the method to non-linear problems (Iturrioz, 1995; Dalguer *et al.*, 2003; Miguel *et al.*, 2008).

Figure 1 shows the critical stress in a homogeneous plate with an edge crack subjected to a uniform tensile stress applied at the upper and lower plate boundaries according to theoretical LEFM and computed using a DEM model by Rocha and Riera (1990). The length of the elements was in all cases equal to 0.01m, size that appears to yield accurate results except in the case of the shortest edge crack, which might require adopting a finer mesh. In such cases, assessing the adequacy of a given mesh presents no difficulty except eventually high computational costs.

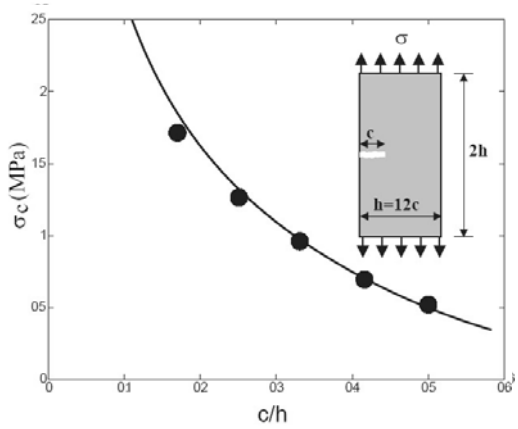

Figure 1: Critical stress for tensile fracture of a rectangular plate (0.12×0.24m) in plane stress with edge crack computed by DEM model (solid dots) and predicted by LEFM (Rocha and Riera, 1990).

A somewhat different situation appears in the solution of problems involving non-homogeneous materials, because in such case the size of the elements must be sufficiently small both in relation to the size of the crack as well as in relation to the correlation lengths of the fields that model the material non-homogeneities. These requirements can rarely be met in engineering practice on account of the resulting computational costs, demanding resort to larger DEM or FEM elements. In this context, the determination of the static strength of rock dowels reported by Miguel *et al.* (2008) is discussed next. In this case a cubic rock dowel fixed at its base is subjected to a uniform tangential stress (shear) at its upper face. Figure 2(a) shows the resulting applied tangential stress *vs.* mean angular distortion of the dowel, computed using five different DEM meshes, ranging from element lengths equal to 0.05m (model with 8000 cubic cells shown in Fig. 2b) to lengths equal to 0.20m (model with only 125 cells shown in Fig.2c). The material in the example was assumed homogeneous, with the

mean properties of granite: Young's modulus $E = 7.5\times10^{10}$Pa, specific fracture energy G_f = 1300N/m, Poisson's ratio $\nu = 0.25$ and mass density $\rho = 2700$kg/m^3. In all cases the analysis predicts the occurrence of fracture starting at the intersection of the dowel with the foundation plane, thus clearly indicating stress localization. The difference between the results obtained with the various models is negligible for engineering purposes, in spite of the coarse mesh adopted in the less dense models.

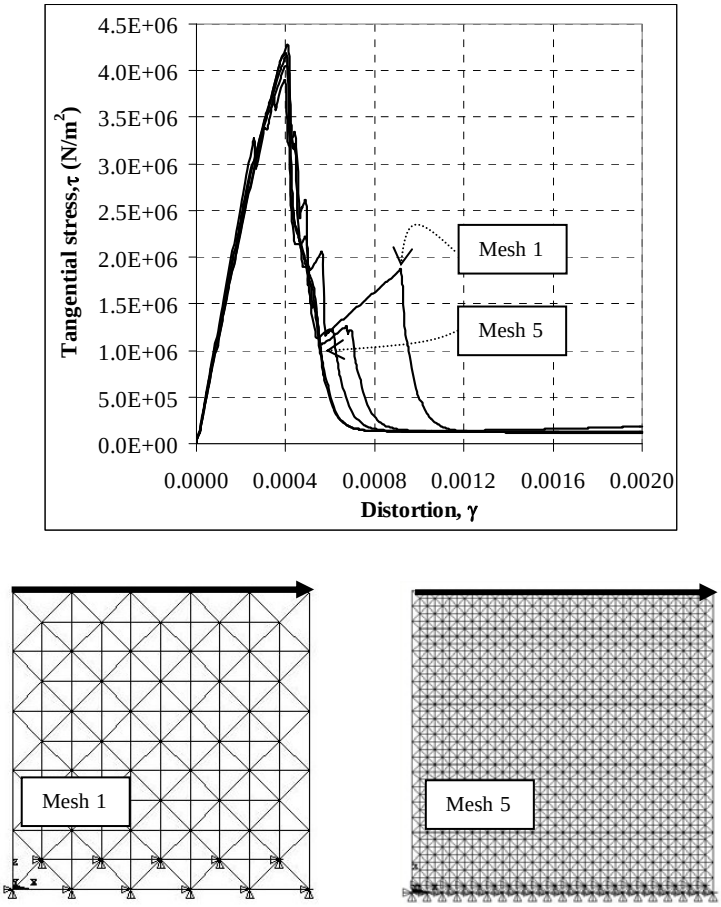

Figure 2: (a) Tangential stress vs. distortion for a 1m cube using five different meshes. (b) Mesh 1: 5×5×5 cubic modules, (c) Mesh 5: 20×20×20.

It may be concluded that the DEM, as employed by the authors for determining the response of homogeneous solids subjected to arbitrary static or dynamic loading, including LEFM problems, is robust and reliable. In case of non-homogeneous materials, the authors obtained solutions by simulation, generating samples of the random fields that define the spatial variation of material properties (Rios and Riera, 2004; Miguel *et al.*, 2008). In such case, the issue of mesh-independence requires a more detailed examination, which is the subject of this paper. The basic features of the DEM in these applications are summarized in Section 2. Examples that cover the full range of possible situations, from strong stress localization to no stress localization are presented in Sections 3 and 4, providing numerical evidence for the conclusions advanced in Section 5.

2 THE DISCRETE ELEMENT METHOD IN FRACTURE PROBLEMS

The Discrete Element Method employed in this paper is based on the representation of a solid by means of an arrangement of elements able to carry only axial loads The equivalence between an orthotropic elastic continuum and the cubic arrangement of uni-axial elements consisting of a cubic cell with eight nodes at its corners plus a central node was shown by Nayfeh and Hefzy (1978). The discrete elements representation of the orthotropic continuum was adopted by the authors to solve structural dynamics problems by means of explicit direct numerical integration of the equations of motion, assuming the mass lumped at the nodes. Each node has three degrees of freedom, corresponding to the nodal displacements in the three orthogonal coordinate directions.

The equivalence between the orthotropic elastic solid with orthotropy axes oriented in the direction parallel to the longitudinal elements of the discrete elements model was extensively verified by Hayashi (1982). The equations that relate the properties of the elements with the elastic constants of an isotropic medium are:

$$\delta = \frac{9\nu}{4-8\nu} \ , \qquad E_A = EA_n = EL_0^2 \frac{(9+8\delta)}{2(9+12\delta)} \ , \qquad EA_d = \frac{2\sqrt{3}}{3} A_n \tag{1}$$

in which E and ν denote Young's modulus and Poisson's ratio, respectively, while A_n and A_d represent the areas of normal and diagonal elements.

The resulting equations of motion may be written in the well-known form:

$$\boldsymbol{M}\ddot{\vec{x}} + \boldsymbol{C}\dot{\vec{x}} + \vec{F}_r(t) - \vec{P}(t) = 0 \tag{2}$$

in which $\vec{x}$ represents the vector of generalized nodal displacements, $\boldsymbol{M}$ the diagonal mass matrix, $\boldsymbol{C}$ the damping matrix, also assumed diagonal, $\vec{F}_r(t)$ the vector of internal forces acting on the nodal masses and $\vec{P}(t)$ the vector of external forces. Obviously, if $\boldsymbol{M}$ and $\boldsymbol{C}$ are diagonal, Equations (2) are not coupled. Then the explicit central finite differences scheme may be used to integrate Equation (2) in the time domain. Since the nodal coordinates are updated at every time step, large displacements can be accounted for in a natural and efficient manner.

Thus, in all cases the integration is performed employing the explicit central finite differences method. Therefore, the integration time step must to be smaller than a critical value Δt_{crit}, which may be estimated as $0.6L_0/\sqrt{E/\rho}$, in which the denominator represents the velocity of propagation of P-waves in an isotropic elastic medium. The numerator denotes the length of the shortest elements in the model, *i.e.*, the diagonal bars.

In the present paper, the relation between tensile stress and strain in the material was assumed to be triangular, as indicated in Figure 3. The limit strain ε_r is determined to satisfy the condition that, upon rupture of the element, once the strain reaches the value ε_r, energy U_{elem} is liberated, according to Equation (3):

$$U_{elem} = \frac{A_f G_f}{L_0} \tag{3}$$

in which A_f is the fractured area bar, L_0 is the normal bar length and G_f is the specific fracture energy that characterized the material toughness.

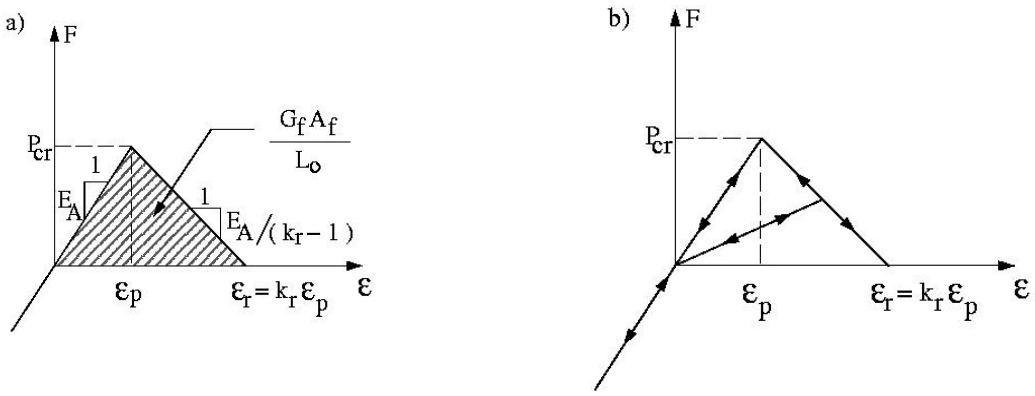

Figure 3: Triangular constitutive law for brittle material.

Note that the fracture energy, *i.e.*, the energy dissipated by the total rupture of one element, depends on the numerator of Equation (3), which is the product of the fracture area *within the element* times the specific fracture energy of the material. In previous papers (Rocha, 1989; Riera and Iturrioz, 1998; Miguel *et al.*, 2008), the assumption that A_f equals the area of the basic brick element L_0^2 was implicit. On that basis, the fracture area of the longitudinal bars is given by:

$$A_f = c_a L_0^2 \tag{4}$$

In which the coefficient c_a was computed as 0.1385. For diagonal bars, c_a equals 0.1593. This assumption is valid as long as there is a strong localization effect, leading to a rupture configuration characterized by a single large crack. One such example is fracture of a rock dowel (Miguel *et al.*, 2008), which occurs in most cases as a crack that, starting near the intersection between the dowel wall and the base, propagates through the dowel. Invariance of the results with different element sizes is shown for such case in Figure 2.

Another important feature of the approach is the assumption that all material properties, such as E and G_f, are not constant throughout the structure. In this paper, a Weibull distribution with coefficient of variation of 25% is adopted for both material properties. It should be underlined again that fracture localization weakens as the non-homogeneous nature of the material becomes more pronounced, *i.e.*, as the coefficients of variation of the fields that describe the material properties increase. On account of this effect, LEFM solutions for plates with edge cracks, such as the theoretical and numerical values shown in Figure 1, for example, are not applicable to non-homogeneous materials like concrete or rock.

Applications of the DEM in studies involving non-homogeneous materials subjected to fracture, like concrete and rock, may be found in Iturrioz (1995), Riera and Iturrioz (1998), Dalguer *et al.* (2001), Rios (2002) and Miguel *et al.* (2008). Additionally, Dalguer *et al.* (2003), Riera *et al.* (2005), Miguel (2005), Miguel *et al.* (2006) and Miguel and Riera (2007), contributed to demonstrate the reliability of the approach.

3 SIZE EFFECT IN FRACTURE ANALYSIS IN NON-HOMOGENEOUS PLATE

Rock plates under plane stress, fixed at their lower face and subjected to tension on their upper face were analyzed up to failure through numerical simulation. The size of the samples ranges from 1.0 to 15.0m. The response of larger specimens may be determined in a similar manner, starting from the constitutive criteria for the individual elements. The smallest array that leads to satisfactory results consists of 10×10×1 cubic modules, with 1026 DOF, used for the 1.0m plate, while the 15.0m plate presents 150×150×1 cubic modules, with 204306 DOF, constituting the largest array used in this study. Table 1 shows the basic dimensions of the four sample sizes analyzed, while Table 2 details the material properties.

Table 1: Basic dimensions of the plate samples.

Plate	L_0	L
Plate 1.0	0.1m	1.0m
Plate 4.0	0.1m	4.0m
Plate 8.0	0.1m	8.0m
Plate 15.0	0.1m	15.0m

Table 2: Properties of brittle materials: granite rock.

Property	Value
E(E) (expected value of Young's modulus)	7.5E10N/m^2
ρ (mass density)	2700kg/m^3
ν (Poisson's ratio)	0.25
E(G_f) (expected value of specific fracture energy)	1300N/m
ε_0 (critical strain)	1.1E-4
CV(E) (coefficient of variation of E)	25%
CV(G_f) (coefficient of variation of G_f)	25%

The nodes on the upper face of the specimens were subjected to controlled displacements that smoothly increase from zero to a limit value. In loading case A, uniform displacements along the upper edge induce a *nominally* uniform tension in the specimen. In loading case B, the test specimens were subjected to a triangularly distributed controlled displacement, inducing a non-uniform tension in the specimen.

Six simulations were carried out for each loading case and for each plate size. The resulting stress-strain curves for all simulations for the 4.0m plate are shown in Figure 4. Note that Young's modulus of the material as well as its fracture energy are regarded as random fields with the properties indicated in Table 2, so each virtual test leads to a different strength and a different stress-strain curve. The mean curve for all simulation is also shown in Figure 4. The mean curves for all tested sizes are shown in Figure 5.

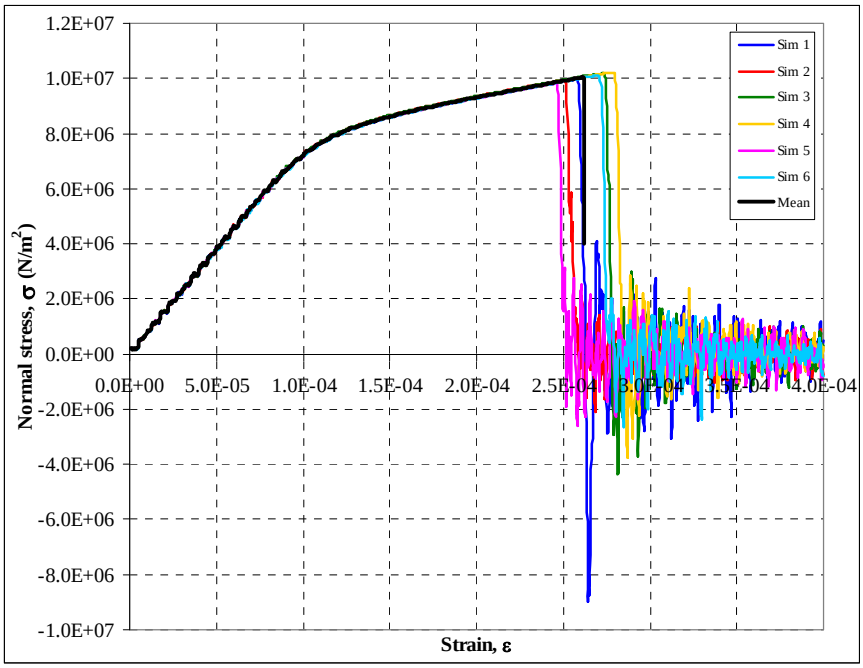

Figure 4: Normal stress on the lower face vs. mean strain for the 4m plate, for all simulations and resulting mean curve (Case A - uniform imposed displacements).

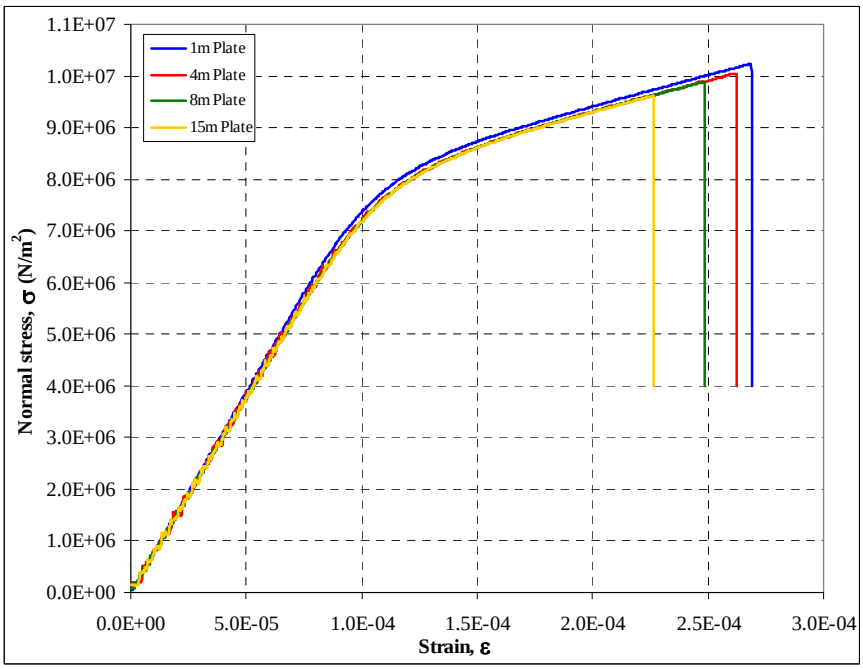

Figure 5: Normal stress on the lower face vs. mean strain for the mean curve of all tested sizes (Case A - uniform imposed displacements).

Next, the plates were subjected to triangularly distributed displacements on their upper face. Six simulations were also performed for each plate size. The resulting stress-strain curves for all simulations for the 4.0m plate are shown in Figure 6, which also presents the mean curve. Figure 7 shows the mean curves for all simulated sample sizes.

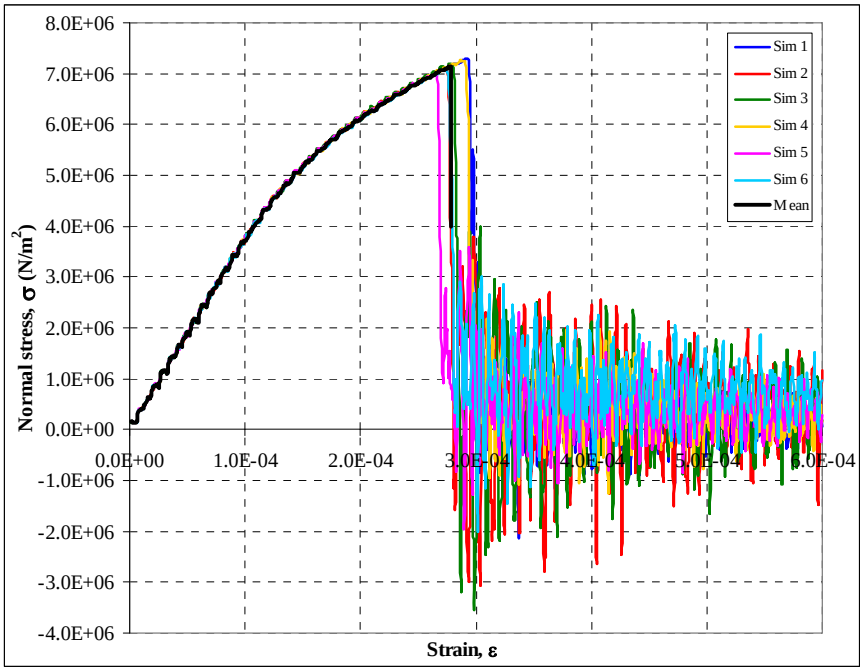

Figure 6: Normal stress on the lower face vs. mean strain for the 4m plate, for all simulations and resulting mean curve (Case B - triangular imposed displacements).

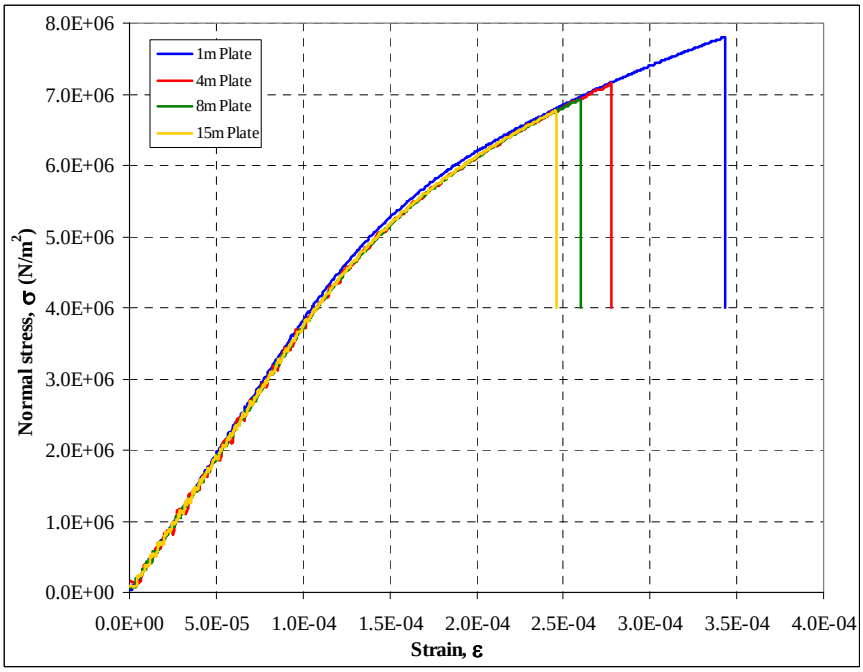

Figure 7: Normal stress on the lower face vs. mean strain for the mean curve of all tested sizes (Case B - triangular imposed displacements).

Typical cracked granite plates in numerical simulation for loading case A are shown in Figure 8, while Figure 9 presents the cracking patterns for case B. In these figures, the colors cyan, orange and red represent the undamaged, damaged and broken elements, respectively.

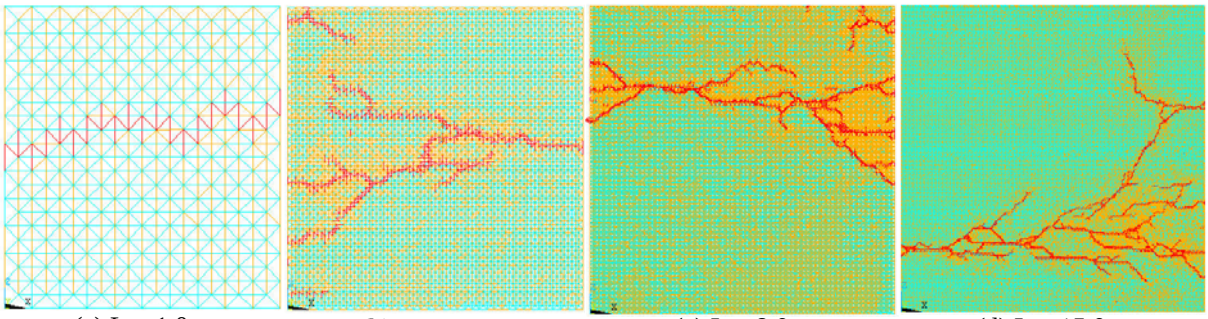

(a) L = 1.0m (b) L = 4.0m (c) L = 8.0m (d) L = 15.0m

Figure 8: Rupture configuration of granite plates subjected to uniform tensile stress (Case A): (a) 1m plate, (b) 4m plate, (c) 8m plate and (d) 15m plate.

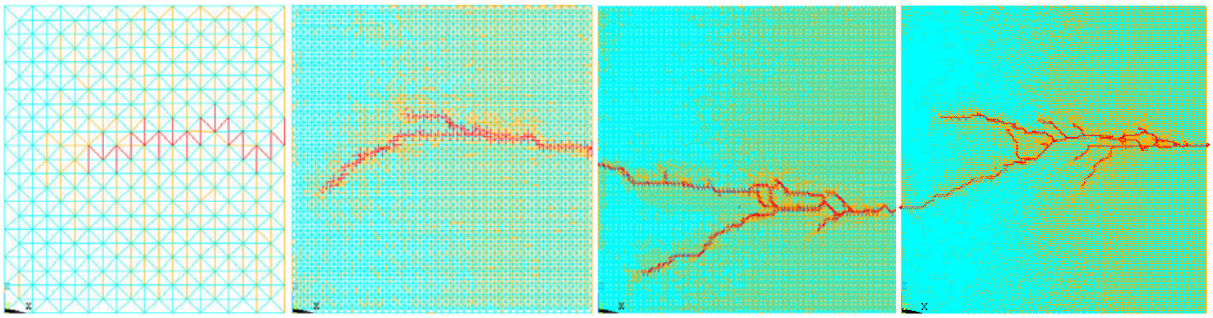

(a) L = 1.0m (b) L = 4.0m (c) L = 8.0m (d) L = 15.0m

Figure 9: Rupture configuration of granite plates subjected to triangular tensile stress (Case B): (a) 1m plate, (b) 4m plate, (c) 8m plate and (d) 15m plate.

The models capture both the size effect as well as cracking patterns, *i.e.*, the damage distribution in the plates. The size effect is clearly visible in Table 3, which illustrates the decrease of the average tensile strength as the size of the plate increases. In Figures 8 and 9 it may be seen that damage localization is more pronounced in presence of a stress gradient (Case B). Both damage, indicated by the orange-tainted regions, as well as crack surfaces are more widely distributed in loading case A (Figure 8). Although no experimental results for this size range are known to the authors, the effects unquestionably exist. Therefore, as discussed later, both features of the non-linear problem should be taken into consideration if larger DEM or FEM elements must be resorted to in order to reduce computational costs.

Table 3: Maximum (rupture) mean tensile stress of simulated plates.

Plate	Case A	Case B
Plate 1.0	10.23MPa	7.80MPa
Plate 4.0	10.04MPa	7.16MPa
Plate 8.0	9.88MPa	6.92MPa
Plate 15.0	9.62MPa	6.77MPa

4 SIZE EFFECT IN FRACTURE ANALYSIS OF LONG ROCK TENDONS

In this section, long rock tendons, fixed at their lower face and subjected to nearly uni-axial tension, were also analyzed up to failure through numerical simulation. The length of the strut specimens ranges from 2.0 to 150.0m. The smallest specimen consists of 20×2×2 cubic modules, with 807 DOF, while the 150.0m tendon presents 1500×2×2 cubic modules. Table 4 shows the basic dimensions of the four sample sizes analyzed, while the material properties are given in Table 2.

Table 4: Basic dimensions of the tendon samples.

Tendon	L_0	L
2.0 long tendon	0.1m	2.0m
50.0 long tendon	0.1m	50.0m
100.0 long tendon	0.1m	100.0m
150.0 long tendon	0.1m	150.0m

The nodes on the upper face of the specimens were subjected to a controlled displacement that increases smoothly from zero up to failure, inducing a nearly uniform tension in the specimen. Six simulations were carried out for each tendon size. The resulting stress-strain curves for all simulations for the 50.0m tendon are shown in Figure 10. The mean curve for all simulation is also shown in Figure 10. The mean curves for all tested tendons are shown in Figure 11.

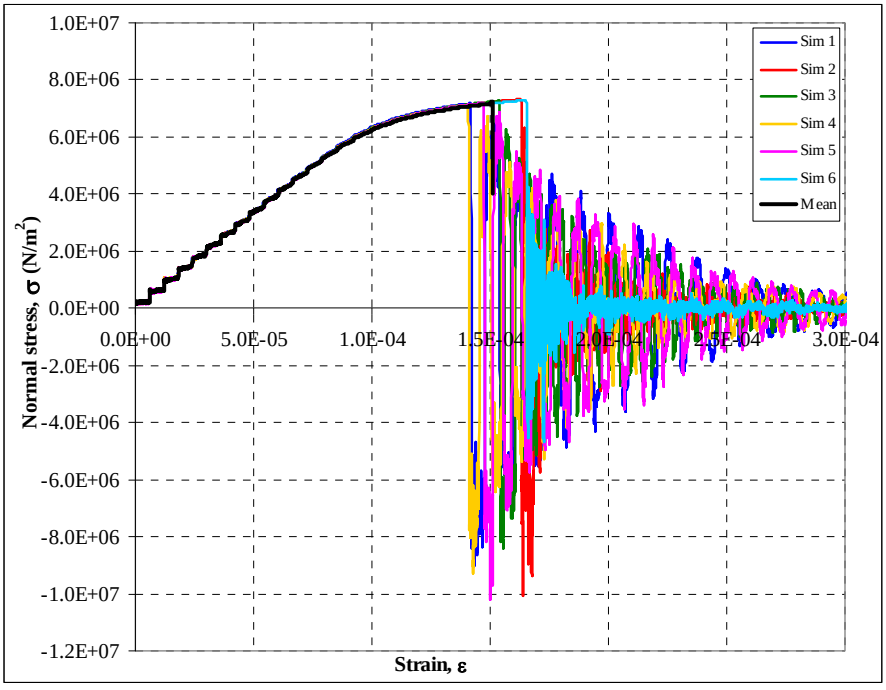

Figure 10: Normal stress on the lower face vs. mean strain for the 50m tendon, for all simulations and resulting mean curve.

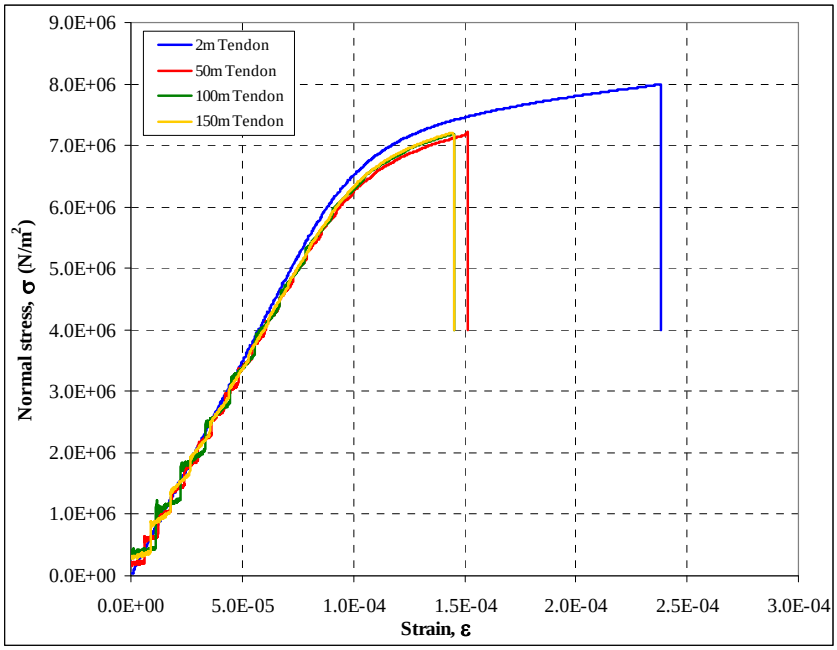

Figure 11: Normal stress on the lower face vs. mean strain for the mean curve of all tested tendons.

In this case, the influence of size on the tendon strength is again quantified by the model, as shown by the decrease of tendon average strength with size, shown in Table 5. Since in an approximately uni-dimensional body, local damage hardly affects the global stress distribution, the problem is much simpler and reduces to the so-called Weibull effect of the strength of materials.

It is important to observe that in some stress-strain curves the simulated response presents severe oscillations after the peak stress is reached, that is, *after rupture*. These oscillations are due to vibrations of fractured regions and as such they are outside the scope of this study.

Table 5: Average tensile strength and corresponding coefficients of variation for the struts.

Tendon	Strength	CV (%)
2.0 long tendon	7.99MPa	4.39
50.0 long tendon	7.22MPa	1.18
100.0 long tendon	7.18MPa	1.44
150.0 long tendon	7.21MPa	2.40

5 ON MESH DEPENDENCE IN DEM FRACTURE PREDICTIONS

The authors correctly quantified size effects in the assessment of rupture of concrete or rock structures subjected to static or dynamic loading employing discrete elements of the same size (Rocha and Riera, 1990; Rios and Riera, 2004; Miguel *et al.*, 2008). In 3-D problems involving large systems, such as NPP containments, dams or rock foundations, larger elements must be resorted to in order to reduce computational costs or to simply render the analysis feasible. Dalguer *et al.* (2003) studied the formation of new cracks in rock layers during an earthquake employing DEM elements with a very large size (several hundred meters) and assumed constitutive relations for rock. Recognizing the need to reliably assess

those relations, for which direct experimental evidence is definitely out of reach, Riera and Iturrioz (2005) suggested the following scheme: determine the constitutive relations of large cubes by simulating tensile tests up to failure of 3-D models, employing for such purpose constitutive elements of a size that *can be tested* in laboratory experiments. By repeating the scheme, the response of very large cubes could be theoretically inferred.

To illustrate the approach, the effective stress-strain curves shown in Figure 5 for plates with sizes ranging from 1.0 to 15.0m will be used. All of them were computed with models consisting of basic 0.1m elements, which are characterized by the stress-strain diagram shown in Figure 3, derived in turn from laboratory tests. Now, it is clear that 1m elements would present the stress-strain curve indicated in blue, while 15m elements would present the curve drawn in yellow (Figure 5). Use of larger elements requires re-evaluation of the properties of the random fields that define material properties, in this case, E and G_f, subject discussed in detail by Riera and Iturrioz (2005). In this reference however, an important issue was not taken into consideration: the energy dissipated in the process of rupture is computed by means of Equation (3) which, if the coefficients c_a indicated in Section 2 are used, implies that only one crack goes through the element. As clearly shown by Figures 8 and 9 and in uncountable laboratory experiments, in large plates or cubes the total fracture surface may largely exceed the minimum fracture surface needed to separate the plate or cube in two parts.

From the preceding reasoning, it is clear that when employing larger elements with length L_0, care must be taken to preserve the energy dissipated in the rupture process, condition the may be satisfied by calculating a new fractured area A_f, as follows:

$$A_f = c_a^* L_0^2 \tag{5}$$

in which the modified coefficient c_a^* must be computed jointly with the evaluation of the effective stress-strain curves for the larger element and represents the ratio between the energy actually dissipated and the minimum energy required to split the element in two parts, given by Equation (3). One difficulty is that the energy depends on the stress field applied, which can be visually confirmed by inspecting Figures 8 and 9. The fractured areas for a given plate size are not the same.

Research is presently under way to develop criteria to predict values of c_a^* for elements of various sizes, which is not an easy task because c_a^* is not independent of the scale of correlation of material properties. It should thus be expected that as size of the element increases, c_a^* will tend to the original c_a values.

6 CONCLUSIONS

It was shown that the prediction of fracture in non-homogeneous materials using DEM models is feasible and yields reliable results. The use of large elements, in which extensive cracking within the basic element of the model may be expected, requires additional research. As applied so far, the approach is successful only in cases where there is intense fracture localization, while tending to underestimate the strength otherwise.

ACKNOWLEDGEMENTS

The authors acknowledge the support of CNPq and CAPES (Brazil).

REFERENCES

Dalguer, L. A., Irikura, K., Riera, J. D., and H. C. Chiu, The importance of the dynamic source effects on strong ground motion during the 1999 Chi-Chi, Taiwan, earthquake: Brief interpretation of the damage distribution on buildings. *Bull. Seismol. Soc. Am.*, 91, 1112-1127, 2001.

Dalguer, L. A., Irikura, K., and Riera, J. D., Simulation of tensile crack generation by three-dimensional dynamic shear rupture propagation during an earthquake. *J. Geophys. Res.*, 108(B3), 2144, 2003.

Hayashi, Y., Sobre uma representação discreta de meios contínuos em dinâmica não-linear. *M. S. thesis*, CPGEC, Universidade Federal do Rio Grande do Sul, Porto Alegre, Brazil, 1982.

Iturrioz, I., Aplicação do método dos elementos discretos ao estudo de estruturas laminares de concreto armado. *Ph.D. thesis*, CPGEC, Universidade Federal do Rio Grande do Sul, Porto Alegre, Brazil, 1995.

Miguel, L. F. F., Critério constitutivo para o deslizamento com atrito ao longo da falha sísmica. *Ph.D. thesis*, 229 pp., PPGEC, Escola de Engenharia, Universidade Federal do Rio Grande do Sul, Porto Alegre, Brazil, 2005.

Miguel, L. F. F., Riera, J. D., and Dalguer, L. A., Macro constitutive law for rupture dynamics derived from micro constitutive law measured in laboratory. *Geophys. Res. Lett.*, 33, L03302, 2006, doi:10.1029/2005GL024912.

Miguel, L. F. F., and Riera, J. D., A constitutive criterion for the fault: modified velocity-weakening law. *Bull. Seismol. Soc. Am.*, 97(3), 915-925, 2007, doi:10.1785/0120060107.

Miguel, L. F. F., Riera, J. D., and Iturrioz, I., Influence of size on the constitutive equations of concrete or rock dowels (Accepted for publication). *International Journal for Numerical and Analytical Methods in Geomechanics*, 2008.

Nayfeh, A. H., and Hefzy, M. S., Continuum modeling of three-dimensional truss-like space structures. *AIAA Journal*, 16(8), 779-787, 1978.

Riera, J. D., and Iturrioz, I., Discrete elements model for evaluating impact and impulsive response of reinforced concrete plates and shells subjected to impulsive loading. *Nuclear Engineering and Design*, 179, 135-144, 1998.

Riera, J. D., and Iturrioz, I., On the fracture analysis of concrete structures taking into consideration size effects. Paper presented at *SMiRT 18: International Conference on Structural Mechanics in Reactor Technology*, Beijing, China, 2005.

Riera, J. D., Miguel, L. F. F., and Dalguer, L. A., On the constitutive criteria for the fault: Influence of size and tensile cracks generation during rupture. Paper presented at *SMiRT 18: International Conference on Structural Mechanics in Reactor Technology*, Beijing, China, 2005.

Rios, R. D., Aplicações do método dos elementos discretos em estruturas de concreto. *Ph.D. thesis*, PPGEC, Universidade Federal do Rio Grande do Sul, Porto Alegre, Brazil, 2002.

Rios, R. D., and Riera, J. D., Size effects in the analysis of reinforced concrete structures. *Engineering Structures*, 26, 1115-1125, 2004.

Rocha, M. M., Ruptura e efeitos de escala em materiais não-homogeneos. *M. S. thesis*, CPGEC, Universidade Federal do Rio Grande do Sul, Porto Alegre, Brazil, 1989.

Rocha, M. M., and J. D. Riera, On size effects and rupture of nonhomogeneous material. In: Van Mier JGM, Rots JG, Baker A, editors. *Proceedings, Congress in Fracture Processes in Concrete, Rock and Ceramics*. London: Chapmen & Hall/Ed. Fn. Spon, p.451-60, 1990.